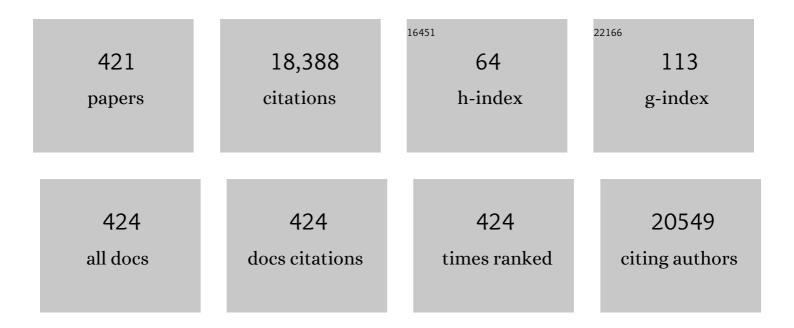
Zi-Feng Yan

List of Publications by Year in descending order

Source: https://exaly.com/author-pdf/6805053/publications.pdf Version: 2024-02-01



71-FENC YAN

#	Article	IF	CITATIONS
1	Review on electrical discharge plasma technology for wastewater remediation. Chemical Engineering Journal, 2014, 236, 348-368.	12.7	752
2	Superior electric double layer capacitors using ordered mesoporous carbons. Carbon, 2006, 44, 216-224.	10.3	690
3	Preparation of highly visible-light active N-doped TiO2 photocatalyst. Journal of Materials Chemistry, 2010, 20, 5301.	6.7	628
4	Recent Advances in Catalysts for Methanol Synthesis via Hydrogenation of CO and CO2. Industrial & Engineering Chemistry Research, 2003, 42, 6518-6530.	3.7	465
5	Superior CO2 uptake of N-doped activated carbon through hydrogen-bonding interaction. Energy and Environmental Science, 2012, 5, 7323.	30.8	434
6	Synthesis and electrochemical properties of mesoporous nickel oxide. Journal of Power Sources, 2004, 134, 324-330.	7.8	331
7	Layered double hydroxides toward high-performance supercapacitors. Journal of Materials Chemistry A, 2017, 5, 15460-15485.	10.3	326
8	Amine-Modified SBA-15: Effect of Pore Structure on the Performance for CO ₂ Capture. Industrial & Engineering Chemistry Research, 2011, 50, 3220-3226.	3.7	240
9	Stable CoSe ₂ /carbon nanodice@reduced graphene oxide composites for high-performance rechargeable aluminum-ion batteries. Energy and Environmental Science, 2018, 11, 2341-2347.	30.8	240
10	Critical role of small micropores in high CO2 uptake. Physical Chemistry Chemical Physics, 2013, 15, 2523.	2.8	228
11	CO2 reforming of CH4 over nanocrystalline zirconia-supported nickel catalysts. Applied Catalysis B: Environmental, 2008, 77, 346-354.	20.2	212
12	Preparation and characterization of SnO2/ZnO/TiO2 composite semiconductor with enhanced photocatalytic activity. Applied Surface Science, 2012, 258, 8704-8712.	6.1	201
13	Influence of chemical functionalization on the CO2/N2 separation performance of porous graphene membranes. Nanoscale, 2012, 4, 5477.	5.6	193
14	Catalytic ammonia decomposition over Ru/carbon catalysts: The importance of the structure of carbon support. Applied Catalysis A: General, 2007, 320, 166-172.	4.3	182
15	Fabrication and Sizeâ€Selective Bioseparation of Magnetic Silica Nanospheres with Highly Ordered Periodic Mesostructure. Advanced Functional Materials, 2008, 18, 3203-3212.	14.9	179
16	Amine-modified mesocellular silica foams for CO2 capture. Chemical Engineering Journal, 2011, 168, 918-924.	12.7	170
17	Superior capacitive performance of active carbons derived from Enteromorpha prolifera. Electrochimica Acta, 2014, 133, 459-466.	5.2	162
18	Recent Advances in the Preparation and Utilization of Carbon Nanotubes for Hydrogen Storage. Journal of Nanoscience and Nanotechnology, 2001, 1, 7-29.	0.9	160

#	Article	IF	CITATIONS
19	Lithiationâ€Induced Vacancy Engineering of Co ₃ O ₄ with Improved Faradic Reactivity for Highâ€Performance Supercapacitor. Advanced Functional Materials, 2020, 30, 2004172.	14.9	156
20	Aqueous dye adsorption on ordered mesoporous carbons. Journal of Colloid and Interface Science, 2007, 310, 83-89.	9.4	154
21	Porous carbons prepared by direct carbonization of MOFs for supercapacitors. Applied Surface Science, 2014, 308, 306-310.	6.1	151
22	High-rate capacitive performance of graphene aerogel with a superhigh C/O molar ratio. Journal of Materials Chemistry, 2012, 22, 23186.	6.7	145
23	Graphene oxide membranes with tunable permeability due to embedded carbon dots. Chemical Communications, 2014, 50, 13089-13092.	4.1	145
24	Anisotropic plasmonic nanostructures for colorimetric sensing. Nano Today, 2020, 32, 100855.	11.9	143
25	One-step solvothermal synthesis of hierarchically porous nanostructured CdS/TiO2 heterojunction with higher visible light photocatalytic activity. Applied Surface Science, 2013, 283, 402-410.	6.1	133
26	Synthesis of mesoporous alumina with highly thermal stability using glucose template in aqueous system. Microporous and Mesoporous Materials, 2006, 91, 293-295.	4.4	132
27	Boosting the bifunctional oxygen electrocatalytic performance of atomically dispersed Fe site via atomic Ni neighboring. Applied Catalysis B: Environmental, 2020, 274, 119091.	20.2	130
28	Nanocrystalline zirconia as catalyst support in methanol synthesis. Applied Catalysis A: General, 2005, 279, 241-245.	4.3	122
29	Extremely enhanced CO2 uptake by HKUST-1 metal–organic framework via a simple chemical treatment. Microporous and Mesoporous Materials, 2014, 183, 69-73.	4.4	122
30	In situ one-step synthesis of Fe3O4@MIL-100(Fe) core-shells for adsorption of methylene blue from water. Journal of Colloid and Interface Science, 2017, 505, 186-195.	9.4	121
31	Syngas Production by Methane Reforming with Carbon Dioxide on Noble Metal Catalysts. Journal of Natural Gas Chemistry, 2006, 15, 327-334.	1.8	112
32	Adsorption Mechanism of Oil by Resilient Graphene Aerogels from Oil–Water Emulsion. Langmuir, 2018, 34, 1890-1898.	3.5	110
33	Study on the photocatalysis of F–S co-doped TiO2 prepared using solvothermal method. Applied Catalysis B: Environmental, 2010, 96, 458-465.	20.2	108
34	Enhanced visible-light activity of F-N co-doped TiO2 nanocrystals via nonmetal impurity, Ti3+ ions and oxygen vacancies. Applied Surface Science, 2013, 287, 135-142.	6.1	106
35	Diffusion and catalyst efficiency in hierarchical zeolite catalysts. National Science Review, 2020, 7, 1726-1742.	9.5	104
36	Electrostatic Self-Assembly of Sandwich-Like CoAl-LDH/Polypyrrole/Graphene Nanocomposites with Enhanced Capacitive Performance. ACS Applied Materials & Interfaces, 2017, 9, 31699-31709.	8.0	103

#	Article	IF	CITATIONS
37	Flexible carbon nanofiber film with diatomic Fe-Co sites for efficient oxygen reduction and evolution reactions in wearable zinc-air batteries. Nano Energy, 2021, 87, 106147.	16.0	103
38	Sustainable and hierarchical porous Enteromorpha prolifera based carbon for CO2 capture. Journal of Hazardous Materials, 2012, 229-230, 183-191.	12.4	102
39	Adsorption and Catalytic Activation of O ₂ Molecule on the Surface of Au-Doped Graphene under an External Electric Field. Journal of Physical Chemistry C, 2012, 116, 19918-19924.	3.1	99
40	Hyper-Branched Cu@Cu ₂ O Coaxial Nanowires Mesh Electrode for Ultra-Sensitive Glucose Detection ACS Applied Materials & Interfaces, 2015, 7, 16802-16812.	8.0	99
41	In-situ ion-activated carbon nanospheres with tunable ultramicroporosity for superior CO2 capture. Carbon, 2019, 143, 531-541.	10.3	96
42	The fabrication of porous N-doped carbon from widely available urea formaldehyde resin for carbon dioxide adsorption. Journal of Colloid and Interface Science, 2014, 416, 124-132.	9.4	95
43	Carbon-encapsulated CoSe nanoparticles derived from metal-organic frameworks as advanced cathode material for Al-ion battery. Journal of Power Sources, 2018, 401, 6-12.	7.8	94
44	Synthesis and Structure Characterization of Chromium Oxide Prepared by Solid Thermal Decomposition Reaction. Journal of Physical Chemistry B, 2006, 110, 178-183.	2.6	92
45	Hierarchically ordered meso/macroporous γ-alumina for enhanced hydrodesulfurization performance. Microporous and Mesoporous Materials, 2012, 158, 1-6.	4.4	89
46	Hydrophobic Functional Group Initiated Helical Mesostructured Silica for Controlled Drug Release. Advanced Functional Materials, 2008, 18, 3834-3842.	14.9	85
47	Fluid catalytic cracking technology: current status and recent discoveries on catalyst contamination. Catalysis Reviews - Science and Engineering, 2019, 61, 333-405.	12.9	84
48	Au@Ag core/shell nanoparticles as colorimetric probes for cyanide sensing. Nanoscale, 2014, 6, 9939-9943.	5.6	83
49	Magnetic metal–organic framework composites for environmental monitoring and remediation. Coordination Chemistry Reviews, 2020, 413, 213261.	18.8	82
50	Low-temperature solvothermal synthesis of visible-light-responsive S-doped TiO2 nanocrystal. Applied Surface Science, 2012, 258, 4016-4022.	6.1	81
51	Hierarchical peony-like FeCo-NC with conductive network and highly active sites as efficient electrocatalyst for rechargeable Zn-air battery. Nano Research, 2020, 13, 1090-1099.	10.4	77
52	CO2 adsorption on Santa Barbara Amorphous-15 (SBA-15) and amine-modified Santa Barbara Amorphous-15 (SBA-15) with and without controlled microporosity. Journal of Colloid and Interface Science, 2013, 390, 217-224.	9.4	74
53	Dispersion of nickel nanoparticles in the cages of metal-organic framework: An efficient sorbent for adsorptive removal of thiophene. Chemical Engineering Journal, 2017, 315, 469-480.	12.7	74
54	Preparation and Characterization of γ-Al ₂ O ₃ with Rich BrÃ,nsted Acid Sites and Its Application in the Fluid Catalytic Cracking Process. Journal of Physical Chemistry C, 2014, 118, 6226-6234.	3.1	72

#	Article	IF	CITATIONS
55	Oxygen-containing functional group-facilitated CO2 capture by carbide-derived carbons. Nanoscale Research Letters, 2014, 9, 189.	5.7	72
56	Orthogonal synthesis, structural characteristics, and enhanced visible-light photocatalysis of mesoporous Fe2O3/TiO2 heterostructured microspheres. Applied Surface Science, 2014, 311, 314-323.	6.1	69
57	Nitrogen and Sulfur Co-Doped Graphene Nanosheets to Improve Anode Materials for Sodium-Ion Batteries. ACS Applied Materials & Interfaces, 2018, 10, 37172-37180.	8.0	69
58	Facile route to prepare bimodal mesoporous γ-Al2O3 as support for highly active CoMo-based hydrodesulfurization catalyst. Applied Catalysis B: Environmental, 2012, 121-122, 50-56.	20.2	68
59	Degradation of organic dye by pulsed discharge non-thermal plasma technology assisted with modified activated carbon fibers. Chemical Engineering Journal, 2013, 215-216, 969-978.	12.7	68
60	Superhigh-rate capacitive performance of heteroatoms-doped double shell hollow carbon spheres. Carbon, 2015, 86, 235-244.	10.3	68
61	Epitaxial growth of hyperbranched Cu/Cu2O/CuO core-shell nanowire heterostructures for lithium-ion batteries. Nano Research, 2015, 8, 2763-2776.	10.4	68
62	Low-temperature synthesis of alkalis doped TiO2 photocatalysts and their photocatalytic performance for degradation of methyl orange. Journal of Alloys and Compounds, 2013, 580, 15-22.	5.5	67
63	Carbon dots functionalized by organosilane with double-sided anchoring for nanomolar Hg2+ detection. Journal of Colloid and Interface Science, 2015, 437, 28-34.	9.4	67
64	Relationship between Surface Chemistry and Catalytic Performance of Mesoporous γ-Al ₂ O ₃ Supported VO <i>_X</i> Catalyst in Catalytic Dehydrogenation of Propane. ACS Applied Materials & Interfaces, 2016, 8, 25979-25990.	8.0	67
65	Insight of synergistic effect of different active metal ions in layered double hydroxides on their electrochemical behaviors. Electrochimica Acta, 2017, 253, 302-310.	5.2	67
66	Copolymer-Controlled Homogeneous Precipitation for the Synthesis of Porous Microfibers of Alumina. Langmuir, 2007, 23, 4599-4605.	3.5	66
67	Catalytic ammonia decomposition over CMK-3 supported Ru catalysts: Effects of surface treatments of supports. Carbon, 2007, 45, 11-20.	10.3	66
68	Direct Synthesis of Water-Dispersible Magnetic/Plasmonic Heteronanostructures for Multimodality Biomedical Imaging. Nano Letters, 2019, 19, 3011-3018.	9.1	66
69	A colorimetric agarose gel for formaldehyde measurement based on nanotechnology involving Tollens reaction. Chemical Communications, 2014, 50, 8121-8123.	4.1	65
70	On the origin of the high capacitance of carbon derived from seaweed with an apparently low surface area. Journal of Materials Chemistry A, 2014, 2, 18998-19004.	10.3	65
71	A review of the direct oxidation of methane to methanol. Chinese Journal of Catalysis, 2016, 37, 1206-1215.	14.0	65
72	Tetragonal nanocrystalline zirconia powder with high surface area and mesoporous structure. Powder Technology, 2006, 168, 59-63.	4.2	64

#	Article	IF	CITATIONS
73	Key parameters in hydrothermal synthesis and characterization of low silicon content SAPO-34 molecular sieve. Microporous and Mesoporous Materials, 2009, 126, 1-7.	4.4	63
74	Microwave- and conventional-hydrothermal synthesis of CuS, SnS and ZnS: Optical properties. Ceramics International, 2013, 39, 4757-4763.	4.8	63
75	Sandwich-like graphene/polypyrrole/layered double hydroxide nanowires for high-performance supercapacitors. Journal of Power Sources, 2016, 331, 67-75.	7.8	62
76	Ammonia assisted functionalization of cuprous oxide within confined spaces of SBA-15 for adsorptive desulfurization. Chemical Engineering Journal, 2018, 339, 557-565.	12.7	62
77	Hierarchical branched Cu ₂ O nanowires with enhanced photocatalytic activity and stability for H ₂ production. Nanoscale, 2014, 6, 195-198.	5.6	61
78	Gold nanoparticles supported on mesoporous silica: origin of high activity and role of Au NPs in selective oxidation of cyclohexane. Scientific Reports, 2016, 6, 18817.	3.3	61
79	Formation of PdO on Au–Pd bimetallic catalysts and the effect on benzyl alcohol oxidation. Journal of Catalysis, 2019, 375, 32-43.	6.2	60
80	Catalytic Ammonia Decomposition over Industrial-Waste-Supported Ru Catalysts. Environmental Science & Technology, 2007, 41, 3758-3762.	10.0	58
81	CO2â^'CH4Reforming over Nickel Catalysts Supported on Mesoporous Nanocrystalline Zirconia with High Surface Area. Energy & Fuels, 2007, 21, 581-589.	5.1	58
82	New strategy to prepare ultramicroporous carbon by ionic activation for superior CO2 capture. Chemical Engineering Journal, 2018, 337, 290-299.	12.7	58
83	Metal and acid sites instantaneously prepared over Ni/SAPO-11 bifunctional catalyst. Journal of Catalysis, 2019, 374, 208-216.	6.2	58
84	Highly stable phosphine modified VOx/Al2O3 catalyst in propane dehydrogenation. Applied Catalysis B: Environmental, 2020, 274, 119089.	20.2	57
85	Self-Assembly of Clewlike ZnO Superstructures in the Presence of Copolymer. Journal of Physical Chemistry C, 2007, 111, 9729-9733.	3.1	56
86	Effects of K ₂ O Promoter on the Activity and Stability of Nickel Catalysts Supported on Mesoporous Nanocrystalline Zirconia in CH ₄ Reforming with CO ₂ . Energy & Fuels, 2008, 22, 2195-2202.	5.1	56
87	Simultaneous removal of NOx and soot particulates over La0.7Ag0.3MnO3 perovskite oxide catalysts. Catalysis Today, 2010, 158, 423-426.	4.4	56
88	Excellent Capacitive Performance of a Threeâ€Dimensional Hierarchical Porous Graphene/Carbon Composite with a Superhigh Surface Area. Chemistry - A European Journal, 2014, 20, 13314-13320.	3.3	56
89	Insight into high areal capacitances of low apparent surface area carbons derived from nitrogen-rich polymers. Carbon, 2015, 94, 560-567.	10.3	56
90	Cation–anion double hydrolysis derived mesoporous γ-Al2O3 as an environmentally friendly and efficient aldol reaction catalyst. Journal of Materials Chemistry, 2009, 19, 1554.	6.7	55

#	Article	IF	CITATIONS
91	Facile synthesis of thermally stable mesoporous crystalline alumina by using a novel cation–anion double hydrolysis method. Materials Letters, 2005, 59, 3128-3131.	2.6	54
92	Ordered mesoporous carbon/Nafion as a versatile and selective solid-phase microextraction coating. Journal of Chromatography A, 2014, 1365, 29-34.	3.7	54
93	Sandwich-like nitrogen-doped porous carbon/graphene nanoflakes with high-rate capacitive performance. Nanoscale, 2016, 8, 7889-7898.	5.6	54
94	Remarkable supercapacitor performance of petal-like LDHs vertically grown on graphene/polypyrrole nanoflakes. Journal of Materials Chemistry A, 2017, 5, 8964-8971.	10.3	53
95	Oriented ZnO nanorods grown on a porous polyaniline film as a novel coating for solid-phase microextraction. Journal of Chromatography A, 2013, 1319, 21-26.	3.7	52
96	Evolution and impact of acidic oxygen functional groups on activated carbon fiber cloth during NO oxidation. Carbon, 2013, 54, 444-453.	10.3	50
97	Phosphorus-modified b-axis oriented hierarchical ZSM-5 zeolites for enhancing catalytic performance in a methanol to propylene reaction. Applied Catalysis A: General, 2020, 594, 117464.	4.3	49
98	In situ FT-IR study of CO and H2 adsorption on a Pt/Al2O3 catalyst. Catalysis Today, 2001, 68, 155-160.	4.4	48
99	Optimizing the sol–gel parameters on the synthesis of mesostructure nanocrystalline γ-Al2O3. Microporous and Mesoporous Materials, 2009, 122, 72-78.	4.4	48
100	A convenient colorimetric method for sensitive and specific detection of cyanide using Ag@Au core–shell nanoparticles. Sensors and Actuators B: Chemical, 2016, 228, 366-372.	7.8	48
101	Boosting the performance of hybrid supercapacitors through redox electrolyte-mediated capacity balancing. Nano Energy, 2020, 68, 104226.	16.0	48
102	Mesoporous nanocrystalline zirconia powders: A promising support for nickel catalyst in CH4 reforming with CO2. Materials Letters, 2007, 61, 2628-2631.	2.6	46
103	A colorimetric assay for measuring iodide using Au@Ag core–shell nanoparticles coupled with Cu2+. Analytica Chimica Acta, 2015, 891, 269-276.	5.4	46
104	Metal-acid balance in the in-situ solid synthesized Ni/SAPO-11 catalyst for n-hexane hydroisomerization. Fuel, 2019, 243, 398-405.	6.4	46
105	Hydro-liquefaction of microcrystalline cellulose, xylan and industrial lignin in different supercritical solvents. Bioresource Technology, 2016, 219, 281-288.	9.6	45
106	Nanocrystalline Zirconia as Support for Nickel Catalyst in Methane Reforming with CO2. Energy & Fuels, 2006, 20, 923-929.	5.1	44
107	Lowâ€Temperature Synthesis of Visible‣ight Active Fluorine/Sulfur Coâ€doped Mesoporous TiO ₂ Microspheres. Chemistry - A European Journal, 2011, 17, 1096-1100.	3.3	44
108	Nitric oxide oxidation catalyzed by microporous activated carbon fiber cloth: An updated reaction mechanism. Applied Catalysis B: Environmental, 2014, 148-149, 573-581.	20.2	44

#	Article	IF	CITATIONS
109	Ultrasmall NiFe layered double hydroxide strongly coupled on atomically dispersed FeCo-NC nanoflowers as efficient bifunctional catalyst for rechargeable Zn-air battery. Science China Materials, 2020, 63, 1182-1195.	6.3	44
110	A rechargeable 6-electron Al–Se battery with high energy density. Energy Storage Materials, 2021, 41, 667-676.	18.0	44
111	Fabrication of Copper Nanowire Encapsulated in the Pore Channels of SBA-15 by Metal Organic Chemical Vapor Deposition. Journal of Physical Chemistry C, 2007, 111, 12536-12541.	3.1	42
112	Soft synthesis of single-crystal coppernanowires of various scales. New Journal of Chemistry, 2012, 36, 130-138.	2.8	42
113	Effects of synthetic conditions on the textural structure of pseudo-boehmite. Journal of Colloid and Interface Science, 2016, 469, 1-7.	9.4	42
114	Pore confinement effect of MoO3/Al2O3 catalyst for deep hydrodesulfurization. Chemical Engineering Journal, 2017, 330, 706-717.	12.7	42
115	Confinement of mesopores within ZSM-5 and functionalization with Ni NPs for deep desulfurization. Chemical Engineering Journal, 2018, 354, 706-715.	12.7	42
116	Enhanced desulfurization characteristics of Cu-KIT-6 for thiophene. Microporous and Mesoporous Materials, 2014, 199, 108-116.	4.4	41
117	Facile fabrication of Ni-based KIT-6 for adsorptive desulfurization. Chemical Engineering Journal, 2016, 302, 239-248.	12.7	41
118	Preparation and application of mesoporous Fe/carbon composites as a drug carrier. Microporous and Mesoporous Materials, 2009, 117, 678-684.	4.4	40
119	A reverse cation–anion double hydrolysis approach to the synthesis of mesoporous γ-Al2O3 with a bimodal pore size distribution. Microporous and Mesoporous Materials, 2009, 118, 288-295.	4.4	40
120	Efficient CO2 capture on low-cost silica gel modified by polyethyleneimine. Journal of Natural Gas Chemistry, 2012, 21, 319-323.	1.8	40
121	Self-assembly of double helical nanostructures inside carbon nanotubes. Nanoscale, 2013, 5, 4191.	5.6	40
122	Facile preparation of Cu–Cu2O nanoporous nanoparticles as a potential catalyst for non-enzymatic glucose sensing. RSC Advances, 2013, 3, 2178.	3.6	40
123	Highly dispersive lanthanum oxide fabricated in confined space of SBA-15 for adsorptive desulfurization. Chemical Engineering Journal, 2020, 384, 123271.	12.7	40
124	Multi-Arch-Structured All-Carbon Aerogels with Superelasticity and High Fatigue Resistance as Wearable Sensors. ACS Applied Materials & Interfaces, 2020, 12, 16822-16830.	8.0	40
125	Copper@carbon coaxial nanowires synthesized by hydrothermal carbonization process from electroplating wastewater and their use as an enzyme-free glucose sensor. Analyst, The, 2013, 138, 559-568.	3.5	39
126	Room temperature hydrogen sensor with ultrahigh-responsive characteristics based on Pd/SnO2/SiO2/Si heterojunctions. Sensors and Actuators B: Chemical, 2016, 227, 438-447.	7.8	39

#	Article	IF	CITATIONS
127	Effect of ethanol on the surface properties and n-heptane isomerization performance of Ni/SAPO-11. Applied Surface Science, 2017, 401, 57-64.	6.1	39
128	Structure and performance of Cu/ZrO2 catalyst For the synthesis of methanol from CO2 hydrogenation. Journal of Fuel Chemistry and Technology, 2010, 38, 462-467.	2.0	38
129	A novel bottom-up solvothermal synthesis of carbon nanosheets. Journal of Materials Chemistry A, 2014, 2, 2390.	10.3	38
130	Size regulation and dispersion of ceria using confined spaces for adsorptive desulfurization. Chemical Engineering Journal, 2018, 348, 319-326.	12.7	38
131	Unusual Pd nanoparticle dispersion in microenvironment for p-nitrophenol and methylene blue catalytic reduction. Journal of Colloid and Interface Science, 2020, 578, 37-46.	9.4	38
132	Outstanding capacitive performance of ordered mesoporous carbon modified by anthraquinone. Electrochimica Acta, 2018, 259, 110-121.	5.2	37
133	Two-stage glucose-assisted crystallization of ZSM-5 to improve methanol to propylene (MTP). Microporous and Mesoporous Materials, 2018, 270, 57-66.	4.4	37
134	Polycyclic Aromatic Hydrocarbons as a New Class of Promising Cathode Materials for Aluminumâ€lon Batteries. Angewandte Chemie - International Edition, 2022, 61, e202114681.	13.8	37
135	Rapid and large-scale synthesis of Cu nanowires via a continuous flow solvothermal process and its application in dye-sensitized solar cells (DSSCs). RSC Advances, 2012, 2, 11544.	3.6	35
136	Excellent membranes for hydrogen purification: Dumbbell-shaped porous Î ³ -graphynes. International Journal of Hydrogen Energy, 2017, 42, 5168-5176.	7.1	35
137	Study of coke deposited on a VO x -K 2 O/ \hat{I}^3 -Al 2 O 3 catalyst in the non-oxidative dehydrogenation of isobutane. Applied Catalysis A: General, 2017, 545, 1-9.	4.3	35
138	Chromium oxide catalysts for COx-free hydrogen generation via catalytic ammonia decomposition. Journal of Molecular Catalysis A, 2009, 304, 71-76.	4.8	34
139	Synthesis of corundum-type In ₂ O ₃ porous spheres and their photocatalytic properties. Journal of Materials Chemistry A, 2014, 2, 5455-5461.	10.3	34
140	Synthesis and catalytic properties of ZSM-5 zeolite with hierarchical pores prepared in the presence of n-hexyltrimethylammonium bromide. Journal of Materials Chemistry A, 2015, 3, 18586-18597.	10.3	34
141	Role of nickel on vanadium poisoned FCC catalyst: A study of physiochemical properties. Journal of Energy Chemistry, 2016, 25, 667-676.	12.9	34
142	Synthesis and characterization of mesoporous Si-modified alumina with high thermal stability. Microporous and Mesoporous Materials, 2017, 238, 84-89.	4.4	34
143	A high surface area mesoporous γ-Al2O3 with tailoring texture by glucose template for ethanol dehydration to ethylene. Microporous and Mesoporous Materials, 2017, 241, 89-97.	4.4	34
144	Oriented freeze-casting fabrication of resilient copper nanowire-based aerogel as robust piezoresistive sensor. Chemical Engineering Journal, 2019, 364, 28-36.	12.7	34

#	Article	IF	CITATIONS
145	Hydrogen storage and release by bending carbon nanotubes. Computational Materials Science, 2013, 68, 121-126.	3.0	33
146	Rapid functionalization of as-synthesized KIT-6 with nickel species occluded with template for adsorptive desulfurization. Microporous and Mesoporous Materials, 2015, 214, 54-63.	4.4	33
147	One-Pot Cation–Anion Double Hydrolysis Derived Ni/ZnO–Al ₂ O ₃ Absorbent for Reactive Adsorption Desulfurization. Industrial & Engineering Chemistry Research, 2016, 55, 3751-3758.	3.7	33
148	Comparison of the Reactive Adsorption Desulfurization Performance of Ni/ZnO–Al ₂ O ₃ Adsorbents Prepared by Different Methods. Energy & Fuels, 2016, 30, 2874-2881.	5.1	33
149	High performance aluminum ion battery using polyaniline/ordered mesoporous carbon composite. Journal of Power Sources, 2020, 477, 228702.	7.8	33
150	Regulation of synergy between metal and acid sites over the Ni-SAPO-11 catalyst for n-hexane hydroisomerization. Fuel, 2020, 274, 117855.	6.4	33
151	Synthesis and characterization of MCM-41-type composite materials prepared from ZSM-5 zeolite. Journal of Porous Materials, 2008, 15, 205-211.	2.6	32
152	Adsorption characteristics of N-nitrosodimethylamine from aqueous solution on surface-modified activated carbons. Journal of Hazardous Materials, 2009, 168, 51-56.	12.4	32
153	Kalsilite based heterogeneous catalyst for biodiesel production. Fuel, 2010, 89, 2163-2165.	6.4	32
154	Outstanding capacitive performance of reticular porous carbon/graphene sheets with superhigh surface area. Electrochimica Acta, 2016, 190, 923-931.	5.2	32
155	Facile functionalization of 3-D ordered KIT-6 with cuprous oxide for deep desulfurization. Chemical Engineering Journal, 2017, 330, 372-382.	12.7	32
156	Highly efficient catalysts of Mn1â^'xAgxCo2O4 spinel oxide for soot combustion. Catalysis Communications, 2017, 101, 134-137.	3.3	32
157	Surface dealumination of micro-sized ZSM-5 for improving propylene selectivity and catalyst lifetime in methanol to propylene (MTP) reaction. Catalysis Communications, 2018, 109, 1-5.	3.3	32
158	Synthesis and Stabilization of Nanocrystalline Zirconia with MSU Mesostructure. Journal of Physical Chemistry B, 2004, 108, 15523-15528.	2.6	31
159	Synthesis of pure tetragonal zirconium oxide with high surface area. Journal of Materials Science, 2007, 42, 1228-1237.	3.7	31
160	Synthesis and hydrodesulfurization performance of hierarchical mesopores alumina. Catalysis Today, 2010, 158, 446-451.	4.4	31
161	New morphological Ba0.5Sr0.5Co0.8Fe0.2O3â~α hollow fibre membranes with high oxygen permeation fluxes. Ceramics International, 2013, 39, 431-437.	4.8	31
162	Functionalization of Petroleum Coke-Derived Carbon for Synergistically Enhanced Capacitive Performance. Nanoscale Research Letters, 2016, 11, 163.	5.7	31

#	Article	IF	CITATIONS
163	Preparation, scale-up and application of meso-ZSM-5 zeolite by sequential desilication–dealumination. Journal of Porous Materials, 2017, 24, 1513-1525.	2.6	31
164	Beta-MCM-41 micro-mesoporous catalysts in the hydroisomerization of n-heptane: Definition of an indexed isomerization factor as a performance descriptor. Microporous and Mesoporous Materials, 2019, 277, 17-28.	4.4	31
165	β-Hydrogen of Polythiophene Induced Aluminum Ion Storage for High-Performance Al-Polythiophene Batteries. ACS Applied Materials & Interfaces, 2020, 12, 46065-46072.	8.0	31
166	High-performance aluminum-polyaniline battery based on the interaction between aluminum ion and -NH groups. Science China Materials, 2021, 64, 318-328.	6.3	31
167	Synthesis and characterization of chromium oxide nanocrystals via solid thermal decomposition at low temperature. Microporous and Mesoporous Materials, 2008, 112, 621-626.	4.4	30
168	Screening of optimum condition for combined modification of ultra-stable Y zeolites using multi-hydroxyl carboxylic acid and phosphate. Catalysis Today, 2010, 158, 198-204.	4.4	30
169	Revisiting the StÓ§ber method: Design of nitrogen-doped porous carbon spheres from molecular precursors of different chemical structures. Journal of Colloid and Interface Science, 2016, 476, 55-61.	9.4	30
170	Improved catalytic cracking performance of USY in the presence of metal contaminants by post-synthesis modification. Fuel, 2016, 178, 243-252.	6.4	30
171	ZSM-5-based mesostructures by combined alkali dissolution and re-assembly: Process controlling and scale-up. Chemical Engineering Journal, 2016, 302, 323-333.	12.7	30
172	Unusual nickel dispersion in confined spaces of mesoporous silica by one-pot strategy for deep desulfurization of sulfur compounds and FCC gasoline. Chemical Engineering Journal, 2017, 321, 48-57.	12.7	30
173	Bifuntional petaloid nickel manganese layered double hydroxides decorated on a freestanding carbon foam for flexible asymmetric supercapacitor and oxygen evolution. Electrochimica Acta, 2017, 252, 275-285.	5.2	30
174	Surfactant assisted electrospinning of WS2 nanofibers and its promising performance as anode material of sodium-ion batteries. Electrochimica Acta, 2019, 302, 259-269.	5.2	30
175	Effect of process parameters on the synthesis of mesoporous nanocrystalline zirconia with triblock copolymer as template. Journal of Porous Materials, 2008, 15, 171-179.	2.6	29
176	Adsorption of bulky molecules of nonylphenol ethoxylate on ordered mesoporous carbons. Journal of Colloid and Interface Science, 2008, 322, 558-565.	9.4	29
177	The enhanced adsorption of sulfur compounds onto mesoporous Ni-AlKIT-6 sorbent, equilibrium and kinetic analysis. Journal of Hazardous Materials, 2014, 270, 82-91.	12.4	29
178	Hydro-liquefaction of sawdust and its three components in supercritical ethanol with [BMIM]Cl/NiCl 2 catalyst. Chemical Engineering Journal, 2015, 279, 921-928.	12.7	29
179	Highly Active Catalyst of Two-Dimensional CoS2/Graphene Nanocomposites for Hydrogen Evolution Reaction. Nanoscale Research Letters, 2015, 10, 488.	5.7	29
180	VOx–K2O∫γ-Al2O3 catalyst for nonoxidative dehydrogenation of isobutane. Fuel Processing Technology, 2016, 151, 31-39.	7.2	29

#	Article	IF	CITATIONS
181	Zeolite Y Mother Liquor Modified γ-Al ₂ O ₃ with Enhanced Brönsted Acidity as Active Matrix to Improve the Performance of Fluid Catalytic Cracking Catalyst. Industrial & Engineering Chemistry Research, 2018, 57, 1389-1398.	3.7	29
182	Perovskite-Type LaCoO ₃ as an Efficient and Green Catalyst for Sustainable Partial Oxidation of Cyclohexane. Industrial & Engineering Chemistry Research, 2020, 59, 21322-21332.	3.7	29
183	Superior catalytic performance of micro-mesoporous Beta-SBA-15 composite with a high indexed isomerization factor in hydroisomerization of n-heptane. Fuel, 2019, 252, 653-665.	6.4	28
184	Revealing the impacting factors of cathodic carbon catalysts for Li-CO2 batteries in the pore-structure point of view. Electrochimica Acta, 2019, 311, 41-49.	5.2	28
185	Fabrication of highly dispersed Pt NPs in nanoconfined spaces of as-made KIT-6 for nitrophenol and MB catalytic reduction in water. Separation and Purification Technology, 2021, 265, 118532.	7.9	28
186	Catalytic decomposition of ammonia over fly ash supported Ru catalysts. Fuel Processing Technology, 2008, 89, 1106-1112.	7.2	27
187	A highly stable catalyst in methane reforming with carbon dioxide. Scripta Materialia, 2009, 61, 173-176.	5.2	27
188	A flexible chemical vapor deposition method to synthesize copper@carbon core–shell structured nanowires and the study of their structural electrical properties. New Journal of Chemistry, 2012, 36, 1161.	2.8	27
189	High performance of H3BO3 modified USY and equilibrium catalyst with tailored acid sites in catalytic cracking. Microporous and Mesoporous Materials, 2017, 243, 319-330.	4.4	27
190	The regulation of Si distribution and surface acidity of SAPO-11 molecular sieve. Applied Surface Science, 2018, 453, 350-357.	6.1	27
191	Vanadium and nickel deposition on FCC catalyst: Influence of residual catalyst acidity on catalytic products. Microporous and Mesoporous Materials, 2019, 273, 276-285.	4.4	27
192	Mechanistic Study of Carbon Dioxide Reforming with Methane over Supported Nickel Catalysts. Energy & Fuels, 1998, 12, 1114-1120.	5.1	26
193	Synthesis of polyaniline-coated ordered mesoporous carbon and its enhanced electrochemical properties. Materials Letters, 2007, 61, 4627-4630.	2.6	26
194	Cation–anion double hydrolysis derived mesoporous γ-Al ₂ O ₃ as an environmentally friendly and efficient aldol reaction catalyst. Journal of Materials Chemistry, 2008, 18, 74-76.	6.7	26
195	Preparation and nitrogen-doping of three-dimensionally ordered macroporous TiO2 with enhanced photocatalytic activity. Ceramics International, 2014, 40, 11213-11219.	4.8	26
196	In-situ synthesis of highly efficient visible light driven stannic oxide/graphitic carbon nitride heterostructured photocatalysts. Journal of Colloid and Interface Science, 2016, 480, 118-125.	9.4	26
197	Effective adsorptive performance of Fe3O4@SiO2 core shell spheres for methylene blue: kinetics, isotherm and mechanism. Journal of Porous Materials, 2019, 26, 1465-1474.	2.6	26
198	Mechanistic insights into structural and surface variations in Y-type zeolites upon interaction with binders. Applied Catalysis A: General, 2019, 571, 137-149.	4.3	26

#	Article	IF	CITATIONS
199	Unraveling the Diffusion Properties of Zeolite-Based Multicomponent Catalyst by Combined Gravimetric Analysis and IR Spectroscopy (AGIR). ACS Catalysis, 2020, 10, 6822-6830.	11.2	26
200	Layered double hydroxides derived NiCo-sulfide as a cathode material for aluminum ion batteries. Electrochimica Acta, 2020, 344, 136174.	5.2	26
201	Single-atom Zn for boosting supercapacitor performance. Nano Research, 2022, 15, 1715-1724.	10.4	26
202	Synthesis of mesoporous alumina TUD-1 with high thermostability. Journal of Porous Materials, 2006, 13, 245-250.	2.6	25
203	Fabrication and Biosensing with CNT/Aligned Mesostructured Silica Coreâ^'Shell Nanowires. ACS Applied Materials & Interfaces, 2010, 2, 2767-2772.	8.0	25
204	Effect of isobutane adsorption on the electrical resistivity of activated carbon fiber cloth with select physical and chemical properties. Carbon, 2014, 76, 435-445.	10.3	25
205	High hydrogen response of Pd/TiO2/SiO2/Si multilayers at room temperature. Sensors and Actuators B: Chemical, 2014, 205, 255-260.	7.8	25
206	Hierarchical SAPO-11 preparation in the presence of glucose. Materials Letters, 2015, 154, 116-119.	2.6	25
207	Effects of dissolution alkalinity and self-assembly on ZSM-5-based micro-/mesoporous composites: a study of the relationship between porosity, acidity, and catalytic performance. CrystEngComm, 2015, 17, 3820-3828.	2.6	25
208	Superior performance of freeze-dried Ni/ZnO-Al 2 O 3 adsorbent in the ultra-deep desulfurization of high sulfur model gasoline. Fuel Processing Technology, 2017, 156, 505-514.	7.2	25
209	Active Sites and Induction Period of Fe/ZSM-5 Catalyst in Methane Dehydroaromatization. ACS Catalysis, 2021, 11, 6771-6786.	11.2	25
210	Synthesis of mesoporous nanocrystalline zirconia with tetragonal crystallite phase by using ethylene diamine as precipitation agent. Journal of Materials Science, 2007, 42, 7086-7092.	3.7	24
211	Effects of CO2 content on the activity and stability of nickel catalyst supported on mesoporous nanocrystalline zirconia. Journal of Natural Gas Chemistry, 2008, 17, 278-282.	1.8	24
212	Particle effect of SAPO-11 promoter on isomerization reaction in FCC units. Microporous and Mesoporous Materials, 2014, 194, 90-96.	4.4	24
213	NO oxidation by microporous zeolites: Isolating the impact of pore structure to predict NO conversion. Applied Catalysis B: Environmental, 2015, 163, 573-583.	20.2	24
214	Enhanced Capacitive Performance of N-Doped Activated Carbon from Petroleum Coke by Combining Ammoxidation with KOH Activation. Nanoscale Research Letters, 2016, 11, 245.	5.7	24
215	Ultrastable bimetallic catalyst with tuned surface electronic properties for highly selective oxidation of cyclohexane. Applied Surface Science, 2018, 457, 580-590.	6.1	24
216	Small graphite nanoflakes as an advanced cathode material for aluminum ion batteries. Chemical Communications, 2020, 56, 1593-1596.	4.1	24

#	Article	IF	CITATIONS
217	Pilot Preparation of Activated Carbon for Natural Gas Storage. Energy & amp; Fuels, 2008, 22, 3420-3423.	5.1	23
218	Furfuralcohol Co-Polymerized Urea Formaldehyde Resin-derived N-Doped Microporous Carbon for CO2 Capture. Nanoscale Research Letters, 2015, 10, 1041.	5.7	23
219	Monte Carlo simulation study of the halogenated MIL-47(V) frameworks: influence of functionalization on H2S adsorption and separation properties. Journal of Materials Science, 2016, 51, 2307-2319.	3.7	23
220	Effect of lanthanum species on the physicochemical properties of La/SAPO-11 molecular sieve. Journal of Catalysis, 2017, 347, 170-184.	6.2	23
221	High performance heterojunction photocatalytic membranes formed by embedding Cu ₂ 0 and TiO ₂ nanowires in reduced graphene oxide. Catalysis Science and Technology, 2018, 8, 1704-1711.	4.1	23
222	Fabrication of 3-D confined spaces with Au NPs: Superior dispersion and catalytic activity. Journal of Colloid and Interface Science, 2019, 540, 371-381.	9.4	23
223	Coordination of Acidic Deep Eutectic Solvent–Chromium Trichloride Catalytic System for Efficient Synthesis of Fructose to 5-Hydroxymethylfurfual. Industrial & Engineering Chemistry Research, 2020, 59, 17554-17563.	3.7	23
224	Understanding the Fundamentals of Microporosity Upgrading in Zeolites: Increasing Diffusion and Catalytic Performances. Advanced Science, 2021, 8, e2100001.	11.2	23
225	The modification of activated carbons and the pore structure effect on enrichment of coalâ€bed methane. Asia-Pacific Journal of Chemical Engineering, 2008, 3, 284-291.	1.5	22
226	Bimodal mesoporous γ-Al2O3: A promising support for CoMo-based catalyst in hydrodesulfurization of 4,6-DMDBT. Materials Letters, 2011, 65, 1765-1767.	2.6	22
227	Direct Liquefaction of Sawdust in Supercritical Alcohol over Ionic Liquid Nickel Catalyst: Effect of Solvents. Energy & Fuels, 2014, 28, 6928-6935.	5.1	22
228	Surface chemistry and catalytic performance of chromia/alumina catalysts derived from different potassium impregnation sequences. Applied Surface Science, 2015, 351, 250-259.	6.1	22
229	Fabrication of gold nanoparticles within hierarchically ZSM-5-based micro-/mesostructures (MMZ) with enhanced stability for catalytic reduction of p-nitrophenol and methylene blue. Separation and Purification Technology, 2021, 254, 117645.	7.9	22
230	Fabrication of a magnetic helical mesostructured silica rod. Nanotechnology, 2008, 19, 435608.	2.6	21
231	Clover leaf-shaped Al2O3 extrudate as a support for high-capacity and cost-effective CO2 sorbent. Journal of Hazardous Materials, 2011, 192, 1505-1508.	12.4	21
232	Zeolite Y synthesized with FCC spent catalyst fines: particle size effect on catalytic reactions. Journal of Porous Materials, 2012, 19, 133-139.	2.6	21
233	Facial synthesis of N-doped microporous carbon derived from urea furfural resin with high CO2 capture capacity. Materials Letters, 2014, 117, 273-275.	2.6	21
234	Efficient hydro-liquefaction of woody biomass over ionic liquid nickel based catalyst. Industrial Crops and Products, 2018, 113, 157-166.	5.2	21

#	Article	IF	CITATIONS
235	Free-standing cotton-derived carbon microfiber@nickel-aluminum layered double hydroxides composite and its excellent capacitive performance. Journal of Alloys and Compounds, 2019, 787, 27-35.	5.5	21
236	Isobutane adsorption with carrier gas recirculation at different relative humidities using activated carbon fiber cloth and electrothermal regeneration. Chemical Engineering Journal, 2019, 360, 1011-1019.	12.7	21
237	Isomerization of $\hat{I}\pm$ -pinene with a hierarchical mordenite molecular sieve prepared by the microwave assisted alkaline treatment. Microporous and Mesoporous Materials, 2020, 299, 110117.	4.4	21
238	Direct synthesis of b-axis oriented H-form ZSM-5 zeolites with an enhanced performance in the methanol to propylene reaction. Microporous and Mesoporous Materials, 2020, 302, 110246.	4.4	21
239	The inner heterogeneity of ZSM-5 zeolite crystals. Journal of Materials Chemistry A, 2021, 9, 4203-4212.	10.3	21
240	Optimizing Oxygen Transport Through La _{0.6} Sr _{0.4} Co _{0.2} Fe _{0.8} O _{3â~î^} Hollow Fiber by Microstructure Modification and Ag/Pt Catalyst Deposition. Energy & Fuels, 2012, 26, 4728-4734.	5.1	20
241	Self-Assembly of Helical Polyacetylene Nanostructures on Carbon Nanotubes. Journal of Physical Chemistry C, 2013, 117, 16248-16255.	3.1	20
242	The preparation, load and photocatalytic performance of N-doped and CdS-coupled TiO2. RSC Advances, 2013, 3, 9483.	3.6	20
243	La _{0.6} Sr _{0.4} Co _{0.2} Fe _{0.8} O _{3â~î^} hollow fibre membrane performance improvement by coating of Ba _{0.5} Sr _{0.5} Co _{0.9} Nb _{0.1} O _{3â~î^} porous layer. RSC Advances, 2014, 4, 19999-20004.	3.6	20
244	Dramatic enhancement of superconductivity in single-crystalline nanowire arrays of Sn. Scientific Reports, 2016, 6, 32963.	3.3	20
245	Growth of copper oxide nanocrystals in metallic nanotubes for high performance battery anodes. Nanoscale, 2016, 8, 19994-20000.	5.6	20
246	Strategy towards enhanced performance of zeolite catalysts: Raising effective diffusion coefficient versus reducing diffusion length. Chemical Engineering Journal, 2020, 385, 123800.	12.7	20
247	One-pot synthesis of the highly efficient bifunctional Ni-SAPO-11 catalyst. Journal of Materials Science and Technology, 2021, 76, 86-94.	10.7	20
248	Adsorption and reusability performance of hierarchically porous silica (MMZ) for the removal of MB dye from water. Inorganic Chemistry Communication, 2022, 139, 109380.	3.9	20
249	Direct hydro-liquefaction of sawdust in petroleum ether and comprehensive bio-oil products analysis. Bioresource Technology, 2014, 155, 152-160.	9.6	19
250	The CO2 Storage Capacity of the Intercalated Diaminoalkane Graphene Oxides: A Combination of Experimental and Simulation Studies. Nanoscale Research Letters, 2015, 10, 1026.	5.7	19
251	Investigation of solvent effect on the hydro-liquefaction of sawdust: An innovative reference approach using tetralin as chemical probe. Fuel, 2016, 164, 94-98.	6.4	19
252	High-performance benzyl alcohol oxidation catalyst: Au-Pd alloy with ZrO2 as promoter. Applied Surface Science, 2021, 537, 148059.	6.1	19

#	Article	IF	CITATIONS
253	Review of Kelvin's Equation and Its Modification in Characterization of Mesoporous Materials. Chinese Journal of Chemical Physics, 2006, 19, 102-108.	1.3	18
254	Tailoring acidity of HZSM-5 nanoparticles for methyl bromide dehydrobromination by Al and Mg incorporation. Nanoscale Research Letters, 2014, 9, 550.	5.7	18
255	Microwave-hydrothermal/solvothermal synthesis of kesterite, an emerging photovoltaic material. Ceramics International, 2014, 40, 1985-1992.	4.8	18
256	Cation–anion double hydrolysis derived mesoporous mixed oxides for reactive adsorption desulfurization. Microporous and Mesoporous Materials, 2017, 238, 36-45.	4.4	18
257	Enhanced dispersion of nickel nanoparticles on SAPO-5 for boosting hydroisomerization of n-hexane. Journal of Colloid and Interface Science, 2021, 604, 727-736.	9.4	18
258	Confinement of Au, Pd and Pt nanoparticle with reduced sizes: Significant improvement of dispersion degree and catalytic activity. Microporous and Mesoporous Materials, 2022, 337, 111927.	4.4	18
259	SYNTHESIS OF NANOCRYSTALLINE MGAL2O4SPINEL BY USING ETHYLENE DIAMINE AS PRECIPITATION AGENT. Chemical Engineering Communications, 2009, 196, 1417-1424.	2.6	17
260	Study on molding semi-coke used for flue-gas desulphurization. Catalysis Today, 2010, 158, 235-240.	4.4	17
261	Effect of vanadium contamination on the framework and micropore structure of ultra stable Y-zeolite. Journal of Colloid and Interface Science, 2016, 463, 188-198.	9.4	17
262	Rapid and green synthesis of SAPO-11 for deoxygenation of stearic acid to produce bio-diesel fractions. Microporous and Mesoporous Materials, 2020, 303, 110280.	4.4	17
263	Mother liquor induced preparation of SAPO-34 zeolite for MTO reaction. Catalysis Today, 2020, 358, 109-115.	4.4	17
264	Improving the performance of lithium ion capacitor by stabilizing anode working potential using CoSe2 nanoparticles embedded nitrogen-doped hard carbon microspheres. Electrochimica Acta, 2021, 370, 137717.	5.2	17
265	Highly dispersive Cu species constructed in mesoporous silica derived from ZSM-5 for batch and continuous adsorptive desulfurization of thiophene. Fuel Processing Technology, 2022, 235, 107351.	7.2	17
266	Synthesis and characterization of mesostructured tungsten nitride by using tungstic acid as the precursor. Journal of Porous Materials, 2006, 13, 173-180.	2.6	16
267	Silicoaluminophosphate-11 (SAPO-11) molecular sieves synthesized <i>via</i> a grinding synthesis method. Chemical Communications, 2018, 54, 10950-10953.	4.1	16
268	Sulfur introduction in V–K/γ-Al ₂ O ₃ catalyst for high performance in the non-oxidative dehydrogenation of isobutane. Catalysis Science and Technology, 2018, 8, 5473-5481.	4.1	16
269	Morphological control in synthesis of cobalt basic carbonate nanorods assembly. Materials Letters, 2008, 62, 1396-1399.	2.6	15
270	Synthesis of ceria doped nanozirconia powder by a polymerized complex method. Journal of Porous Materials, 2009, 16, 497-505.	2.6	15

#	Article	IF	CITATIONS
271	Multi-cationic layered double hydroxides: Calcined products as photocatalysts for decomposition of NOx. Applied Clay Science, 2013, 80-81, 390-397.	5.2	15
272	Synthesis of hierarchical SAPO-11 for hydroisomerization reaction in refinery processes. Applied Petrochemical Research, 2014, 4, 351-358.	1.3	15
273	Detailed investigation of N-doped microporous carbons derived from urea furfural resin for CO2 capture. Journal of Porous Materials, 2015, 22, 1663-1672.	2.6	15
274	Location and Surface Species of Fluid Catalytic Cracking Catalyst Contaminants: Implications for Alleviating Catalyst Deactivation. Energy & amp; Fuels, 2016, 30, 10371-10382.	5.1	15
275	Soluble starch as in-situ template to synthesize ZSM-5 zeolite with intracrystal mesopores. Materials Letters, 2016, 164, 543-546.	2.6	15
276	The structure of alkyl ester sulfonate surfactant micelles: The impact of different valence electrolytes and surfactant structure on micelle growth. Journal of Colloid and Interface Science, 2019, 557, 124-134.	9.4	15
277	Enhanced Supercapacitive Performance of MnCO ₃ @rGO in an Electrolyte with KI as Additive. ChemElectroChem, 2019, 6, 316-319.	3.4	15
278	Enhancing hydrogen oxidation electrocatalysis of nickel-based catalyst by simultaneous chemical anchoring and electronic structure regulation. Chemical Engineering Journal, 2021, 425, 130654.	12.7	15
279	Influence of framework Al distribution in HZSM-5 channels on catalytic performance in the methanol to propylene reaction. Applied Catalysis A: General, 2022, 629, 118422.	4.3	15
280	Fatigue Resistant Aerogel/Hydrogel Nanostructured Hybrid for Highly Sensitive and Ultrabroad Pressure Sensing. Small, 2022, 18, e2104706.	10.0	15
281	MoO ₃ Nanorods Decorated by PbMoO ₄ Nanoparticles for Enhanced Trimethylamine Sensing Performances at Low Working Temperature. ACS Applied Materials & Interfaces, 2022, 14, 24610-24619.	8.0	15
282	Structure characterization of the Co and Ni catalysts for carbon dioxide reforming of methane. Catalysis Today, 2001, 68, 135-143.	4.4	14
283	A novel method to synthesize super-activated carbon for natural gas adsorptive storage. Journal of Porous Materials, 2006, 13, 399-405.	2.6	14
284	Synthesis and characterization of turbostratic carbons prepared by catalytic chemical vapour decomposition of acetylene. Applied Catalysis A: General, 2006, 309, 201-209.	4.3	14
285	The investigation of a hydro-thermal method to fabricate Cu@C coaxial nanowires and their special electronic transport and heat conduction properties. New Journal of Chemistry, 2012, 36, 1255.	2.8	14
286	Desulfurization of Saudi Arabian crudes by oxidation–extraction method. Applied Petrochemical Research, 2015, 5, 355-362.	1.3	14
287	Synthesis of ZSM-5 zeolite from diatomite for fluid catalytic cracking (FCC) application. Applied Petrochemical Research, 2015, 5, 347-353.	1.3	14
288	Narrow-bandgap Nb2O5 nanowires with enclosed pores as high-performance photocatalyst. Science China Materials, 2019, 62, 203-210.	6.3	14

#	Article	IF	CITATIONS
289	Impact of molecular structure, headgroup and alkyl chain geometry, on the adsorption of the anionic ester sulfonate surfactants at the air-solution interface, in the presence and absence of electrolyte. Journal of Colloid and Interface Science, 2019, 544, 293-302.	9.4	14
290	Compatibility between Activity and Selectivity in Catalytic Oxidation of Benzyl Alcohol with Au–Pd Nanoparticles through Redox Switching of SnO <i>_x</i> . ACS Applied Materials & Interfaces, 2021, 13, 49780-49792.	8.0	14
291	Formation of an ink-bottle-like pore structure in SBA-15 by MOCVD. Chemical Communications, 2008, , 5131.	4.1	13
292	Fabrication of copper (I) nitride nanorods within SBA-15 by metal organic chemical vapor deposition. Science in China Series D: Earth Sciences, 2009, 52, 352-356.	0.9	13
293	Synthesis of high surface area \hat{I}^3 -Al2O3 as an efficient catalyst support for dehydrogenation of n-dodecane. Journal of Porous Materials, 2010, 17, 85-90.	2.6	13
294	An efficient modification of ultra-stable Y zeolites using citric acid and ammonium fluosilicate. Applied Petrochemical Research, 2014, 4, 373-378.	1.3	13
295	Functionalized activated carbon prepared form petroleum coke with high-rate supercapacitive performance. Journal of Materials Research, 2016, 31, 3723-3730.	2.6	13
296	Polydopamine-coated graphene nanosheets as efficient electrocatalysts for oxygen reduction reaction. RSC Advances, 2018, 8, 16044-16051.	3.6	13
297	Natural gas storage on activated carbon modified by metal oxides. Journal of Porous Materials, 2009, 16, 27-32.	2.6	11
298	In situ synthesis, characterization and catalytic activity of ZSM-5 zeolites on kaolin microspheres from amine-free system. Journal of Porous Materials, 2013, 20, 137-141.	2.6	11
299	Comprehensive evaluation of hydro-liquefaction characteristics of lignocellulosic subcomponents. Journal of the Energy Institute, 2020, 93, 1705-1712.	5.3	11
300	Impact of γ-alumina pore structure on structure and performance of Ni–Mo/γ-Al2O3 catalyst for 4,6-dimethyldibenzothiophene desulfurization. Microporous and Mesoporous Materials, 2021, 310, 110637.	4.4	11
301	Highly stable Ni/ <scp>ZnOâ€Al₂O₃</scp> adsorbent promoted by <scp>TiO₂</scp> for reactive adsorption desulfurization. EcoMat, 2021, 3, e12114.	11.9	11
302	Relieving hydrogen evolution and anodic corrosion of aqueous aluminum batteries with hybrid electrolytes. Journal of Materials Chemistry A, 2022, 10, 4739-4748.	10.3	11
303	Realizing an aqueous sodium-ion battery with a super-high discharge voltage based on a novel FeSe ₂ @rGO anode. Inorganic Chemistry Frontiers, 2022, 9, 1622-1629.	6.0	11
304	Fabrication of copper nanorods by low-temperature metal organic chemical vapor deposition. Science Bulletin, 2006, 51, 2662-2668.	1.7	10
305	Synthesis and characterization of Mâ€ZSMâ€5 composites prepared from ZSMâ€5 zeolite. Asia-Pacific Journal of Chemical Engineering, 2008, 3, 275-283.	1.5	10
306	Promotion Effects of Nickel Catalysts of Dry Reforming with Methane. Chinese Journal of Chemistry, 2001, 19, 738-744.	4.9	10

#	Article	IF	CITATIONS
307	Effect of Si/Al ratio of the starting NaY on hydro-upgrading catalyst performance. Catalysis Today, 2010, 158, 409-414.	4.4	10
308	Synthesis of Al-MCM-41 and FCC diesel hydrorefining study. Journal of Porous Materials, 2012, 19, 473-479.	2.6	10
309	Preparation of Cu/ZrO2 catalysts for methanol synthesis from CO2/H2. Frontiers of Chemical Science and Engineering, 2012, 6, 47-52.	4.4	10
310	Combined modification of ultra-stable Y zeolites via citric acid and phosphoric acid. Applied Petrochemical Research, 2014, 4, 343-349.	1.3	10
311	The application of mesoporous alumina with rich Brönsted acidic sites in FCC catalysts. Applied Petrochemical Research, 2014, 4, 367-372.	1.3	10
312	Insights into the H2/CH4 Separation Through Two-Dimensional Graphene Channels: Influence of Edge Functionalization. Nanoscale Research Letters, 2015, 10, 492.	5.7	10
313	A colorimetric approach for measuring mercuric ions with high selectivity using label-free gold nanoparticles and thiourea. Analytical Methods, 2015, 7, 6837-6841.	2.7	10
314	Efficient Hydroliquefaction of Sawdust over a Novel Silica-Supported Monoclinic Molybdenum Dioxide Catalyst. Energy & Fuels, 2016, 30, 6495-6499.	5.1	10
315	In-Depth Insight into the Chemical Composition of Bio-oil from Hydroliquefaction of Lignocellulosic Biomass in Supercritical Ethanol with a Dispersed Ni-Based Catalyst. Energy & Fuels, 2016, 30, 5269-5276.	5.1	10
316	Combined alkali dissolution and re-assembly approach toward ZSM-5 mesostructures with extended lifetime in cumene cracking. Journal of Colloid and Interface Science, 2018, 529, 283-293.	9.4	10
317	Intra-crystalline mesoporous SAPO-11 prepared by a grinding synthesis method as FCC promoters to increase iso-paraffin of gasoline. Microporous and Mesoporous Materials, 2020, 305, 110320.	4.4	10
318	In Situ Catalysis and Extraction Approach for Fast Evaluation of Heterogeneous Catalytic Efficiency. Analytical Chemistry, 2020, 92, 9989-9996.	6.5	10
319	Effect of fluoride ions on the stability of SAPO-11 molecular sieves. Microporous and Mesoporous Materials, 2020, 306, 110461.	4.4	10
320	Controllable synthesis of SAPO-11/5 intergrowth zeolite for hydroisomerization of n-hexane. Microporous and Mesoporous Materials, 2021, 313, 110857.	4.4	10
321	Palladium nanoparticles decorated on ZSM-5 derived micro-/mesostructures (MMZ) for nitrophenol reduction and MB degradation in water. Journal of Environmental Chemical Engineering, 2021, 9, 105002.	6.7	10
322	Magnetic rod-based metal-organic framework metal composite as multifunctional nanostirrer with adsorptive, peroxidase-like and catalytic properties. Chinese Chemical Letters, 2021, 32, 3245-3251.	9.0	10
323	Highly dispersive palladium nanoparticle in nanoconfined spaces for heterogeneous catalytic reduction of anthropogenic pollutants. Journal of Colloid and Interface Science, 2021, 594, 304-315.	9.4	10
324	Multivalent cationic and anionic mixed redox of an Sb ₂ S ₃ cathode toward high-capacity aluminum ion batteries. Journal of Materials Chemistry A, 2022, 10, 10829-10836.	10.3	10

#	Article	IF	CITATIONS
325	Effect of the Addition of Antifoulant Agents on the Deactivation of NiMoP/Al2O3 Catalysts for Hydrotreating of Residuum. Industrial & Engineering Chemistry Research, 2000, 39, 3679-3687.	3.7	9
326	A facile one step synthesis of alumina monolith with bimodal pore structure from emulsion template. Materials Letters, 2012, 68, 234-236.	2.6	9
327	Preparation of hierarchical SAPO-11 molecular sieve and its application for n-dodecane isomerization. Applied Petrochemical Research, 2014, 4, 401-407.	1.3	9
328	Remarkably high performance of clew-like ZnO superstructure in reactive adsorption desulfurization. Science China Materials, 2017, 60, 985-994.	6.3	9
329	Predicting Catalytic Performance of Micro-Mesoporous Pt/Beta-KIT-6 Catalyst in <i>n</i> -Heptane Hydroisomerization Using Indexed Isomerization Factor and Experimental Verification. Industrial & Engineering Chemistry Research, 2019, 58, 5146-5157.	3.7	9
330	Multivalent electrolyte induced surface ordering and solution self-assembly in anionic surfactant mixtures: Sodium dodecyl sulfate and sodium diethylene glycol monododecyl sulfate. Journal of Colloid and Interface Science, 2020, 565, 567-581.	9.4	9
331	The effect of co-feeding ethanol on a methanol to propylene (MTP) reaction over a commercial MTP catalyst. Applied Catalysis A: General, 2020, 592, 117429.	4.3	9
332	Mesostructured cellular foam silica supported Au–Pt nanoalloy: Enrichment of d-state electrons for promoting the catalytic synergy. Microporous and Mesoporous Materials, 2021, 316, 110982.	4.4	9
333	Ultrafast and Long-Cycle Stable Aluminum Polyphenylene Batteries. ACS Applied Materials & Interfaces, 2022, 14, 30927-30936.	8.0	9
334	Perspective on FCC catalyst in China. Applied Petrochemical Research, 2013, 3, 63-70.	1.3	8
335	SO2 abatement over nanocrystalline MgAl2O4 spinel-supported catalysts. Journal of Porous Materials, 2013, 20, 571-577.	2.6	8
336	Highly hydrothermally stable Al-MCM-41 with accessible void defects. Journal of Porous Materials, 2013, 20, 309-317.	2.6	8
337	Synthesis of hierarchically ordered egg-tray-like macroporous TiO2–SiO2 nanocomposites with ordered mesoporous walls. Materials Letters, 2013, 111, 173-176.	2.6	8
338	Large-scale synthesis of Cu nanowires with gradient scales by using "hard―strategies and size effects on electrical properties. CrystEngComm, 2013, 15, 332-342.	2.6	8
339	Preparation and hydrodesulfurization properties of cobalt–molybdenum–phosphorous catalysts for removal of dibenzothiophene. Applied Petrochemical Research, 2015, 5, 405-411.	1.3	8
340	Biomimetic fabrication of highly ordered laminae–trestle–laminae structured copper aero-sponge. Nanoscale, 2020, 12, 8982-8990.	5.6	8
341	One-pot green synthesis of Fe-ZSM-5 zeolite containing framework heteroatoms via dry gel conversion for enhanced propylene selectivity of catalytic cracking catalyst. Journal of Materials Science, 2021, 56, 18050-18060.	3.7	8
342	Passivated Surface of High Aluminum Containing ZSM-5 by Silicalite-1: Synthesis and Application in Dehydration Reaction. ACS Sustainable Chemistry and Engineering, 2022, 10, 4839-4848.	6.7	8

#	Article	IF	CITATIONS
343	Role of Nanosized Zirconia on the Properties of Cu/Ga2O3/ZrO2 Catalysts for Methanol Synthesis. Chinese Journal of Chemistry, 2006, 24, 172-176.	4.9	7
344	Enhanced electrochemical properties of polyaniline-coated multiwall carbon nanotubes. Journal of Porous Materials, 2008, 15, 647-651.	2.6	7
345	Effect of potassium carbonate on catalytic synthesis of calcium carbide at moderate temperature. Frontiers of Chemical Science and Engineering, 2011, 5, 372-375.	4.4	7
346	Hydro-liquefaction of woody biomass for bio-oil in supercritical solvent with [BMIM]Cl/NiCl2 catalyst. Applied Petrochemical Research, 2015, 5, 363-369.	1.3	7
347	Synthesis of vanadium-based catalysts and their excellent catalytic behaviors on dehydrogenation of C4 hydrocarbons. Applied Petrochemical Research, 2015, 5, 321-327.	1.3	7
348	Functionalization of petroleum coke-based mesoporous carbon for synergistically enhanced capacitive performance. Journal of Materials Research, 2017, 32, 1248-1257.	2.6	7
349	Vanadium contamination of FCC catalyst: Understanding the destruction and passivation mechanisms. Applied Catalysis A: General, 2018, 555, 108-117.	4.3	7
350	Enhanced Catalytic Performance of the FCC Catalyst with an Alumina Matrix Modified by the Zeolite Y Structure-Directing Agent. Industrial & Engineering Chemistry Research, 2019, 58, 5455-5463.	3.7	7
351	A Generalized Approach to the Synthesis of Mesoporous Mixed Metal Oxides Using the Cation-Anion Double Hydrolysis Method. Science of Advanced Materials, 2011, 3, 994-1003.	0.7	7
352	Polycyclic Aromatic Hydrocarbons as a New Class of Promising Cathode Materials for Aluminumâ€lon Batteries. Angewandte Chemie, 2022, 134, .	2.0	7
353	Effect of heating profile on desorption curve in temperature programmed desorption analysis: case study of acid sites distribution of SAPO-34. Journal of Porous Materials, 2009, 16, 599-603.	2.6	6
354	In situ synthesis of low silica X zeolite on ceramic honeycombs for adsorption of heavy metals. Journal of Porous Materials, 2013, 20, 1525-1529.	2.6	6
355	Studies in the capacitance properties of diaminoalkane-intercalated graphene. Electrochimica Acta, 2014, 148, 220-227.	5.2	6
356	Substituting effect of Ce ³⁺ on the AlPO-11 molecular sieve. Catalysis Science and Technology, 2016, 6, 3821-3831.	4.1	6
357	Effective performance of CeO2 based silica for preparation of octanal. Journal of Porous Materials, 2020, 27, 1101-1108.	2.6	6
358	One-step synthesis of egg-tray-like layered ordered macro-mesoporous SiO2–Al2O3 composites for enhanced hydrodesulfurization performance. Microporous and Mesoporous Materials, 2021, 322, 111131.	4.4	6
359	Elucidation of active species and reaction mechanism of sulfide V-K/Al2O3 catalyst for isobutane dehydrogenation. Applied Surface Science, 2021, 569, 151106.	6.1	6
360	Surface catalysis gaseous nitriding of alloy cast iron at lower temperature. Catalysis Today, 2010, 158, 205-208.	4.4	5

#	Article	IF	CITATIONS
361	Transesterification of soybean oil to biodiesel over kalsilite catalyst. Frontiers of Chemical Science and Engineering, 2011, 5, 325-329.	4.4	5
362	Modification of USY zeolites with malic–nitric acid for hydrocracking. Applied Petrochemical Research, 2016, 6, 353-359.	1.3	5
363	Promoter effect of heteroatom substituted AlPO-11 molecular sieves in hydrocarbons cracking reaction. Journal of Colloid and Interface Science, 2018, 528, 330-335.	9.4	5
364	What is the effect of Sn and Mo oxides on gold catalysts for selective oxidation of benzyl alcohol?. New Journal of Chemistry, 2019, 43, 2591-2599.	2.8	5
365	Deactivation behavior investigation on commercial precipitated iron Fischer–Tropsch catalyst for long time reaction. Journal of Porous Materials, 2022, 29, 307-315.	2.6	5
366	Direct synthesis of nanorod stacked "nest-like―hierarchical ZSM-48 hollow spheres using a triazine-based bolaform organic structure-directing agent. Inorganic Chemistry Frontiers, 2022, 9, 2016-2022.	6.0	5
367	Dual carbon Li-ion capacitor with high energy density and ultralong cycling life at a wide voltage window. Science China Materials, 2022, 65, 2373-2384.	6.3	5
368	A core–shelled Sb@C nanorod cathode with a graphene aerogel interlayer for high-capacity aluminum ion batteries. Nanoscale, 2022, 14, 10566-10572.	5.6	5
369	CNTs/mesostructured silica core-shell nanowires via interfacial surfactant templating. Science Bulletin, 2009, 54, 516-520.	9.0	4
370	Comparative studies of three kinds of activated carbon reactivated by KOH. Asia-Pacific Journal of Chemical Engineering, 2012, 7, 598-603.	1.5	4
371	Soft-templating pathway to create nanostructured Mg–Al spinel as high-temperature absorbent for SO2. Journal of Porous Materials, 2014, 21, 947-956.	2.6	4
372	Prediction on miscibility of silicone and gasoline components by Monte Carlo simulation. Journal of Molecular Modeling, 2014, 20, 2244.	1.8	4
373	One-step synthesis of three-dimensionally ordered macro–mesoporous silica–alumina composites. Materials Letters, 2014, 121, 212-214.	2.6	4
374	Preparation and characterization of hierarchical USY by post-treatment. Applied Petrochemical Research, 2015, 5, 313-319.	1.3	4
375	A comparative study of different fluorine-containing compounds in the preparation of novel alumina binders with rich BrA¶nsted acid sites. Applied Petrochemical Research, 2015, 5, 81-87.	1.3	4
376	A Simple, Rapid and Eco-Friendly Approach for the Analysis of Aromatic Amines in Environmental Water Using Single-Drop Microextraction-Gas Chromatography. Journal of Chromatographic Science, 2015, 53, 360-365.	1.4	4
377	Comment on "Ultrahigh Performance Supercapacitor from Lacey Reduced Graphene Oxide Nanoribbons†ACS Applied Materials & Interfaces, 2016, 8, 26427-26428.	8.0	4
378	Catalytic removal of soot particles over MnCo2O4 catalysts prepared by the auto-combustion method. Chemical Papers, 2018, 72, 1973-1979.	2.2	4

#	Article	IF	CITATIONS
379	3. Functional catalysts for catalytic removal of formaldehyde from air. , 2019, , 89-126.		4
380	Hydrothermal synthesis of beta zeolite from industrial silica sol as silicon source. Journal of Porous Materials, 2019, 26, 1017-1025.	2.6	4
381	α-Sulfo alkyl ester surfactants: Impact of changing the alkyl chain length on the adsorption, mixing properties and response to electrolytes of the tetradecanoate. Journal of Colloid and Interface Science, 2021, 586, 876-890.	9.4	4
382	Direct Synthesis of Nanosheetâ€Stacked Hierarchical "Honey Stickâ€like―MFI Zeolites by an Aromatic Heterocyclic Dualâ€Functional Organic Structureâ€Directing Agent. Chemistry - A European Journal, 2021, 27, 8694-8697.	3.3	4
383	Multivalent counterion induced multilayer adsorption at the air-water interface in dilute Aerosol-OT solutions. Journal of Colloid and Interface Science, 2021, 597, 223-232.	9.4	4
384	Honeycomb-like rGO aerogels via oriented freeze-drying as efficient organic solvents removing absorbents. Materials Letters, 2022, 318, 132164.	2.6	4
385	Modulation of surface chemistry by boron modification to achieve a superior VOX/Al2O3 catalyst in propane dehydrogenation. Catalysis Today, 2022, 402, 248-258.	4.4	4
386	Synthesis of novel ordered carbon nanorods and its application in electrochemical double layer capacitor. Science in China Series D: Earth Sciences, 2006, 49, 425-433.	0.9	3
387	Study on the Desulfurization of High-Sulfur Crude Oil by the Electrochemical Method. Energy & Fuels, 2015, 29, 6928-6934.	5.1	3
388	Effect of SiO2/Al2O3Ratio on Micro-Mesopore Formation for Pt/Beta-MCM-41 via NaOH Treatment and the Catalytic Performance in N-heptane Hydro isomerization. IOP Conference Series: Earth and Environmental Science, 2018, 108, 042105.	0.3	3
389	Catalytic reduction of nitrophenol and MB waste water using homogeneous Pt NPs confined in hierarchically porous silica. Journal of Environmental Chemical Engineering, 2021, 9, 105567.	6.7	3
390	Isobutane dehydrogenation over high-performanced sulfide V-K/γ-Al2O3 catalyst: Modulation of vanadium species and intrinsic effect of potassium. Journal of Colloid and Interface Science, 2021, 600, 440-448.	9.4	3
391	Preparation of Ultrafine Y Zeolite from Spent Fluid Catalytic Cracking Catalyst Powders. Chinese Journal of Catalysis, 2010, 31, 833-838.	14.0	3
392	A novel method to prepare mesoporous nano-zirconia. Studies in Surface Science and Catalysis, 2003, , 239-242.	1.5	2
393	Deactivation study of CoAPO-11 molecular sieve on skeletal isomerization of 1-hexene. Progress in Natural Science: Materials International, 2005, 15, 52-55.	4.4	2
394	Evaporation-controlled nanocasting approach to a precision replication at nanometer scale. Materials Letters, 2007, 61, 4231-4234.	2.6	2
395	Solid-state synthesis and characterisation of mesoporous zirconia with lamellar and wormhole-like mesostructures. Journal of Porous Materials, 2008, 15, 237-244.	2.6	2
396	Hydrogen adsorption on NiNaY composites at room and cryogenic temperatures. Catalysis Today, 2010, 158, 317-323.	4.4	2

#	Article	IF	CITATIONS
397	Perspective on Sustainable Energy Technologies in Asia and Pacific States. Energy & Fuels, 2010, 24, 3713-3714.	5.1	2
398	Ethyl 4-anilino-2,6-bis(4-chlorophenyl)-1-phenyl-1,2,5,6-tetrahydropyridine-3-carboxylate. Acta Crystallographica Section E: Structure Reports Online, 2013, 69, 0947-0948.	0.2	2
399	Synthesis of meso-SAPO-11 and its enhancement of isomerization in fluid catalytic cracking process. Applied Petrochemical Research, 2014, 4, 389-394.	1.3	2
400	Polypyrrole/silver coaxial nanocables structured aerogels as piezoresistive sensors. Materials Letters, 2020, 279, 128474.	2.6	2
401	One-Pot Synthesis of Silica Supported Au–Ag Alloy Nanoparticles for Cyclohexane Oxidation. Nanoscience and Nanotechnology Letters, 2016, 8, 972-977.	0.4	2
402	Catalytic Dehydrogenation of Propane to Propene: Catalyst Development, Mechanistic Aspects and Reactor Design. Reviews in Advanced Sciences and Engineering, 2014, 3, 180-195.	0.6	2
403	Multi-Arches Structured All-Carbon Aerogels with Super Elasticity and High Fatigue Resistance As Sensitive Wearable Sensors. ECS Meeting Abstracts, 2020, MA2020-01, 1978-1978.	0.0	2
404	Advances in porous materials for petrochemical processing: Chinese perspectives. Journal of Porous Materials, 2008, 15, 115-117.	2.6	1
405	Mechanism of forming an ink-bottle-like pore structure based on SBA-15 by a novel MOCVD technique. Science Bulletin, 2010, 55, 446-451.	1.7	1
406	Salt-assisted synthesis of tree-like oriented SnO2 nanodendrite. Frontiers of Chemical Science and Engineering, 2011, 5, 227-230.	4.4	1
407	A simple hydrothermal route to bimodal mesoporous nanorod γ-alumina with high thermal stability. International Journal of Materials Research, 2011, 102, 1473-1476.	0.3	1
408	1,5-Bis(2-methoxybenzylidene)thiocarbonohydrazide methanol monosolvate. Acta Crystallographica Section E: Structure Reports Online, 2013, 69, o1147-o1147.	0.2	1
409	Vacuum ultraviolet photofragmentation of octadecane: photoionization mass spectrometric and theoretical investigation. Applied Petrochemical Research, 2015, 5, 305-311.	1.3	1
410	Synthesis of monodispersed colloidal particles via a hydrothermally promoted double hydrolysis approach. CrystEngComm, 2017, 19, 552-561.	2.6	1
411	Co-assembly route to facile synthesis of hierarchical core-shell nano-CuMOR@SBA-15 composite for one-step conversion of DME to ethanol with enhanced catalytic performance. Journal of Porous Materials, 2020, 27, 855-862.	2.6	1
412	Synthesis and characterization of supersurface MCM-41 zeolite using additives. Studies in Surface Science and Catalysis, 2003, 146, 153-156.	1.5	0
413	Fabrication of Copper Nanowire Encapsulated in SBA-15 Nanocomposite by Metal Organic Chemical Vapor Deposition. , 2006, , .		0
414	Investigation of N-(Hydroxylethyl)pyrrolidone Dehydration over REOx-doped Nano-ZrO2 Catalyst. Chinese Journal of Chemical Engineering, 2006, 14, 309-313.	3.5	0

#	Article	IF	CITATIONS
415	Perspective on catalysis for sustainable energy and environmental technologies. Catalysis Today, 2010, 158, 197.	4.4	0
416	Sucrose-Template Synthesis of Mesoporous Alumina from Aqueous Systems. International Journal of Food Engineering, 2010, 6, .	1.5	0
417	The Influence of Introduction of Polyethylene Glycol on Synthesis of Bimodal Mesoporous γ-Al ₂ O ₃ . Advanced Materials Research, 2013, 709, 89-92.	0.3	0
418	Preface for the special issue of the 1st Saudi–Chinese Oil Refinery Forum (1st SCORF 2013). Applied Petrochemical Research, 2014, 4, 325-327.	1.3	0
419	Preface to the special issue of the "2nd Saudi-Chinese Oil Refinery Forum (SCORF)†advances in multiple catalytic strategies for producing cleaner fuels and petrochemicals. Applied Petrochemical Research, 2015, 5, 245-246.	1.3	0
420	Significant role of ultramicropores on capacitive properties of polypyrrole-based carbons. AIP Conference Proceedings, 2017, , .	0.4	0
421	Copolymer Assisted Self-Assembly of Nanoporous Mixed Oxides for Reactive Adsorption Desulfurization, Nanoscience and Nanotechnology Letters, 2016, 8, 931-937.	0.4	0